

# A heap-based algorithm for the study of one-dimensional particle systems

Alain Noullez<sup>†</sup>, Duccio Fanelli<sup>‡</sup>, Erik Aurell<sup>‡,\*</sup>

<sup>†</sup> *CNRS, Observatoire de la Côte d'Azur,  
B.P. 4229, F-06304 Nice Cedex 4, France*

<sup>‡</sup> *Dept. of Numerical Analysis and Computer Science,  
KTH, SE-100 44 Stockholm, Sweden*

<sup>\*</sup> *Dept. of Mathematics, Stockholm University,  
SE-106 91 Stockholm, Sweden*

---

A fast algorithm to study one-dimensional self-gravitating systems, and, more generally, systems that are Lagrangian integrable between collisions, is presented. The algorithm is event-driven, and uses a heap-ordered set of predicted future events. In the limit of large number of particles  $N$ , the operation count is dominated by the cost of reordering the heap after each event, which goes asymptotically as  $\log N$ . Some applications are discussed in detail.

---

## 1. INTRODUCTION

In this paper we discuss a fast algorithm which integrates numerically a one-dimensional system of  $N$  interacting particles, provided the dynamics can be Lagrangian integrated between two successive collisions. An important application is self-gravitating systems, since the gravitational force is Lagrangian invariant in one dimension. Several similar models with Lagrangian invariant or quasi-invariant force fields can also be treated.

By computing all possible collision times between particles, we can select the smallest of these and let the particles evolve until this time is reached. The particles are then made to collide according to the prescriptions of the dynamics. It is clear that in such a scheme the most time-consuming operation is the search of the minimal collision time. In one dimension, the number of possible collisions between  $N$  particles is  $N - 1$ , because the set of positions is well-ordered. This seems to imply immediately an  $\mathcal{O}(N)$  operations count for each collision. Indeed, if we order the set of collision times, finding the minimum takes  $\mathcal{O}(1)$  operations, but inserting a new collision time in the list will take  $\mathcal{O}(N)$  operations. On the other hand, if we keep the set unordered, adding a new element will take  $\mathcal{O}(1)$  operations, but finding the minimum will take  $\mathcal{O}(N)$ . The essence of an efficient algorithm is to use a data structure that simultaneously permits fast insertion and fast search of the minimum. This is exactly the aim of the heap structure, well known in algorithmic design [6, 7, 16]. Although known since a rather long time, it is only recently that

the heap concept has been used in physical problems, like front propagation [17] or molecular dynamics simulations of hard-sphere systems [9, 10, 13]. In this paper we extend this technique to systems with force fields acting between collisions, provided these fields are Lagrangian invariant, or quasi-invariant.

The paper is organized as follows. In section 2 we introduce the concept of a heap [6], and discuss code speed implementation issues. Section 3 shows how an efficient event-driven evolution scheme can be implemented by using the heap structure. In section 4, we apply this code to the numerical solution of two different one-dimensional systems of particles: the free streaming motion, i.e. the evolution of  $N$  non-interacting particles, and a classical self-gravitating system [12, 18, 19]. This section also contains checks on the speed of the algorithm. In the conclusion section, we sum up our results and discuss future applications.

## 2. THE HEAP

The discussion in this section mainly follows [6], the classical references on the subject being [7, 16].

The *heap* structure is based on the concept of a tree. A tree is formally defined to be a set of *nodes*, connected by *links*, such that the path to go from one node to another is unique. A *rooted tree* is a tree with distinguished node, *the root*, which is usually by convention drawn on the top. A rooted tree can be defined recursively as follows: a rooted tree consists of a root node, and a finite set of subtrees, which are themselves rooted trees. Every node has a unique *parent*, except the root. The *children* of a node  $i$  are the roots of the subtrees, under  $i$ . A node which has no children is called a *leaf*, and is usually drawn at the bottom. Binary trees are the most commonly used: they consist of a root node and at most two subtrees which are themselves binary trees.

A binary tree of  $N$  elements is labeled  $T(N)$ . The nodes can be graded in levels. The children of a node on level  $l$  are on level  $l - 1$ . The height  $h$  is a lower bound on the number of levels needed to build a binary tree of  $N$  elements, with  $h = \lceil \log_2 N \rceil + 1$ , as is illustrated in figure 1. In the following we will use *complete* and *left-justified* binary trees, which are such that all the leaves are on level 2 or 1, and those on level 1 are drawn from the left. The nodes in a complete and left-justified binary tree can be numbered from the top to the bottom, and left to right, such that the children of node  $i$  are respectively  $2i$  and  $2i + 1$ , while its parent (if any) is  $\lfloor i/2 \rfloor$ . Such a tree can be represented by an array with the array index equal to the node number in the tree.

In a *heap-ordered* tree, an element is associated to each node, and the elements obey the *heap condition*: each element in a child node is greater than or equal to the elements in its parent node. An array representing a tree satisfying the heap condition is called a *heap* [7, 16].

Given  $N$  objects, the following strategy can be used to put them in a heap: the first element is placed on the top of the tree, which corresponds to the first element

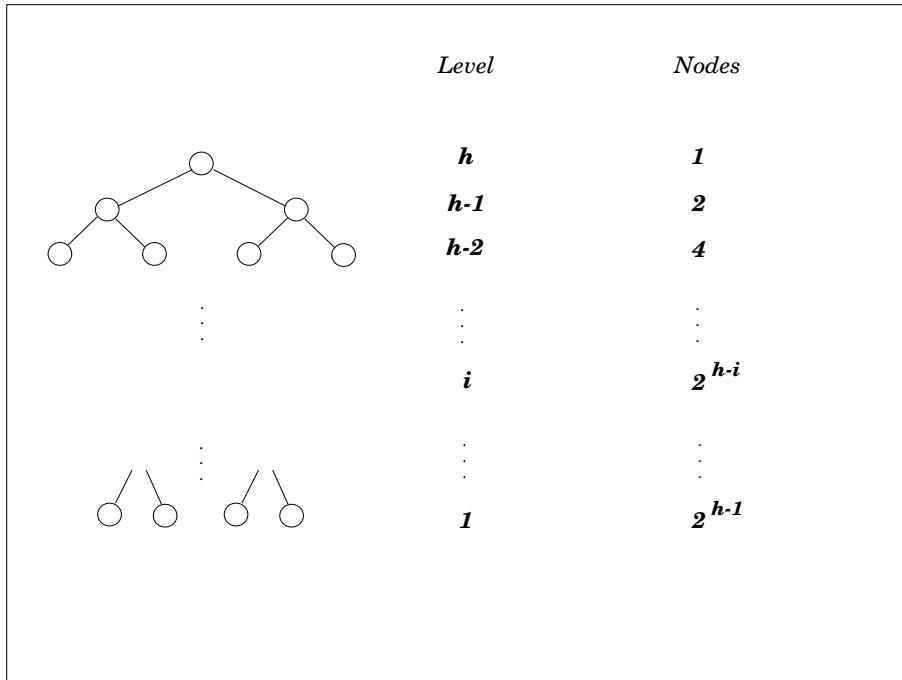


FIG. 1. Example of an ordered complete binary tree.

of the array. The next element is placed in the second position, and after comparison eventually replaces the first, if smaller. This operation is called *sift-up* [16]<sup>1</sup>.

This procedure is iterated: a new entry is placed at the end of the array, and a comparison with its parent is performed. If smaller, the element is exchanged with the parent and is again compared to its new parent, and so on. As a result, each new element moves on an ascending path on the tree until the heap condition is satisfied.

The above described simple procedure to initially order an array in a heap (bottom-up) takes  $\mathcal{O}(N \log N)$  operations at the most. A faster scheme (top-down), that only takes  $\mathcal{O}(N)$  operations in the worst case is however possible [7, 16]. Moreover, once the heap is built, the operational cost of inserting or substituting a new element in a heap is at most  $\mathcal{O}(\log N)$ , the height of the tree, and the selection of the minimum is a trivial  $\mathcal{O}(1)$  operation. The heap is therefore a well adapted data structure for both finding a minimum and replacing elements in an array.

In many applications, elements have to be sorted according to different criteria. It is thus not possible to put them in a single heap, and it would be very inefficient to duplicate data in different heaps. The solution to this problem is to use a single instance of all elements (that might already be sorted itself according to one criterion), and to use *indirect* heap(s) containing only pointers to them [16].

<sup>1</sup>The inverse operation (*sift-down*) makes an element move down through the tree (percolate) until the heap condition is restored. This operation is typically needed when the heap has to be re-ordered after replacement of an element.

When comparing elements while moving through the heap, we access them through the (current) heap pointers and, if the elements don't satisfy the heap condition, we simply exchange their pointers without moving the elements themselves. This procedure can be very efficient if elements carry lots of related data, but it leads to a large amount of memory traffic while moving through the heap, because of the need to indirect through the pointers (but see below).

The concept of trees, and thus of heaps, can be generalized to bases larger than two [8]. In a base  $r$  tree, each node has at most  $r$  subtrees so that, in a complete left-justified  $r$ -ary tree, the children of node  $i$  are  $ri + 2 - r, \dots, ri + 1$  while the parent of node  $i$  is  $\lfloor (i - 2 + r)/r \rfloor = \lceil (i - 1)/r \rceil$ . It is now clear that we face two conflicting requirements: on one hand, we would like to minimize the height of the tree  $h = \log_r N$  by choosing  $r$  as large as possible; on the other hand, the work needed at each level of the tree to find the smallest of the children, e.g. in a sift-down, increases linearly with  $r$ , so we would like to keep it small. Blind minimization of the expression  $r \log_r N$  suggests that the best branching ratio would be  $e$ , the base of natural logarithms. However, the processing of each level also incurs some work independent of  $r$ , and it is thus better to choose some higher (integer) value. This becomes even more important on modern microprocessors that access memory through *caches* which are filled in bursts of typically 4, 8, or 16 words. Because the children of a node are stored consecutively in memory, it is then possible to use the fetching of a cache line to load all children of one node at the same time. This however also requires the heap to be *cache-aligned* [8], which can be realized by fiddling with the base address returned by the memory allocation routines in a language like C. On the microprocessors we used (Alpha, Pentium, MIPS), we found that base 4 was much better than base 2, while bases 8 and higher were slightly slower than base 4. The gain in speed by using aligned base 4 heaps with respect to unaligned base 2 ones is significant, about 25% on a Pentium with 15% coming from the choice of base and 10% from the memory alignment.

To get all the benefits of aligned large base heaps, the comparison keys have to be really present in the heap and not accessed through pointers that would incur extra memory loads. We thus implemented *semi-indirect* heaps in which the keys are placed inside of the heap, so they can be compared directly, while pointers to the corresponding elements are located in an array parallel to the heap. Because pointers have to be exchanged only when doing a swap, this implementation reduces nearly by half the number of memory accesses (to at most  $r + 1$  memory loads and 3 memory writes if a swap occurs in a sift-down) and is faster than other priority queue implementations like those described in [9].

### 3. THE ALGORITHM

We consider the motion of  $N$  colliding particles in a one-dimensional medium. The interaction is not specified at this level: we only require that the equation of motion for a particle can be integrated in between two successive collisions. Arrays of size  $N$  contain the states of the particles, such as position, velocity and acceleration, at the time of their last collision, stored in increasing order of the spatial coordinates. An additional state variable associated to each particle is  $\tau_j$ , the time it last experienced a collision. Initially all  $\tau_j$  are set to zero.

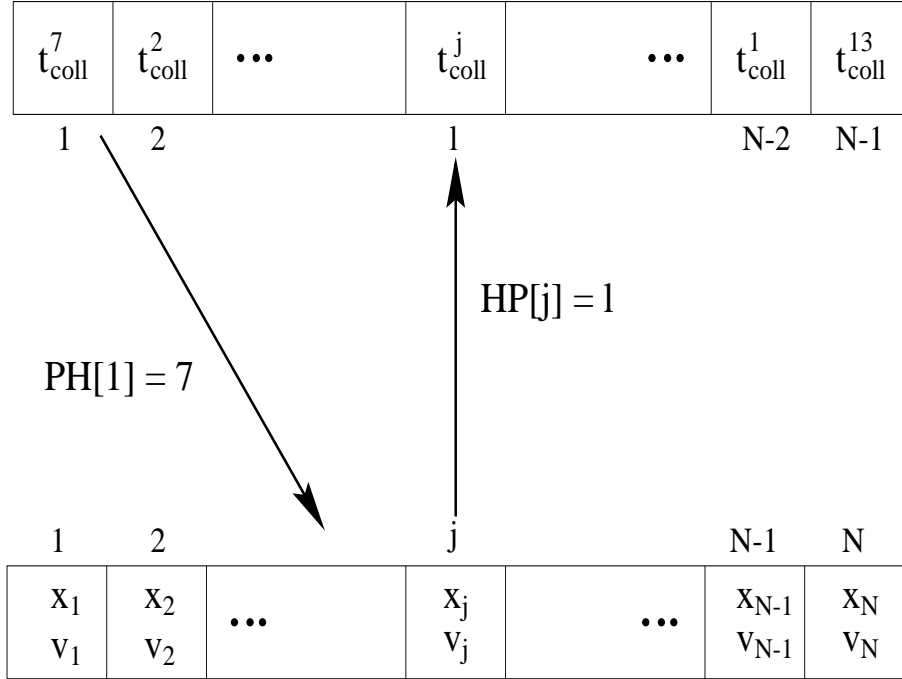


**FIG. 2.** This figure shows the structure of a semi-indirect heap and the function of the two “shuffling” arrays  $PH[\bullet]$  and  $HP[\bullet]$ . The first array in the figure only contains the predicted collision times ordered as a heap, while the second contains the particle states stored in increasing order of spatial positions. The two indexing arrays allow to move back and forth between the two sets.

The algorithm starts by computing the collision time of each particle with its neighbor to the right, and the results are stored in an array of size  $N - 1$ . This array is then turned into a heap,  $T(N - 1)$ . So that we do not need to move the whole states of particles while processing the heap, we introduce an indexing array, Particle-Heap ( $PH[\bullet]$ ), mapping the position in the heap to the position in space. Referring to figure 2 if index  $l$  labels the position of the collision time in the heap, then  $j = PH[l]$  is the index in space of the leftmost of the two particles ( $j$  and  $j + 1$ ) involved in that collision. To update the list of predicted collision times of neighbors particles, we also need the index array inverse to Particle-Heap, which we call Heap-Particle ( $HP[\bullet]$ ). Hence for all  $j$  in the range 1 to  $N - 1$

$$PH[HP[j]] = j \quad \text{and} \quad HP[PH[j]] = j. \quad (1)$$

This condition will be preserved at all times while we update the heap. Note that the collision times are really directly present in the heap, and that the two indexing arrays then realize exactly the functions needed to implement the semi-indirect heap.

The initial forming of the heap requires  $\mathcal{O}(N)$  operations, as stated in the previous section. Once the heap has been built, the minimum collision time  $t_{\text{min}}$  is at the root. The particles involved in the first collision, which are  $j = PH[1]$  and  $j + 1$ , are selected, and their states evolved up to  $t_{\text{min}}$ . The two particles are then at the same spatial position and their states are rearranged by the collision (momenta simply

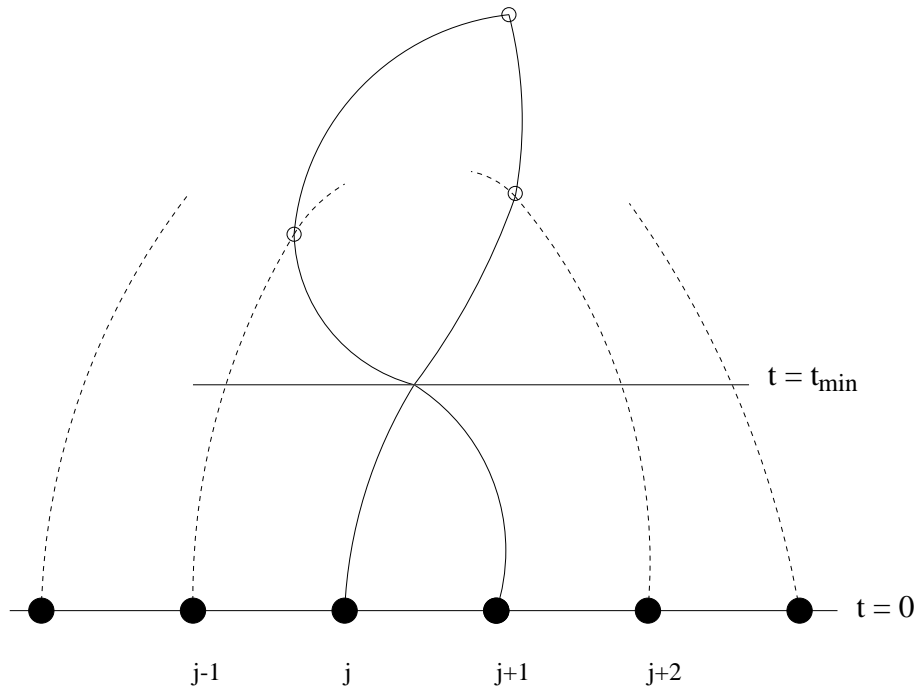


**FIG. 3.** Intersection of the trajectories of particles  $j$  and  $j+1$  at time  $t = t_{\min}$ . The ringed intersections are the collision/crossings that need to be recomputed.

exchanged in the case of elastic collision). The times  $\tau_j$  and  $\tau_{j+1}$ , are set equal to  $t_{\min}$ . This procedure conserves the monotonicity of the particle positions both at and after the collision. Next the new predicted collision times between  $j$  and  $j+1$  is computed and replaces the one at the root of the tree. The root might now not fulfill the heap condition, so the array probably has to be re-arranged with a sift-down of the root value. We need to check whether the new value is still less than the values in its children. If this is not the case, it is percolated down the tree until the heap condition is satisfied. This procedure involves at most  $\mathcal{O}(\log N)$  operations, as discussed previously.

Because of the changes of the states of particles  $j$  and  $j+1$ , their collisions with their other nearest neighbors,  $j-1$  and  $j+2$  need to be re-computed, see figure 3. To do this, particles  $j-1$  and  $j+2$  are temporarily moved forward in time up to  $t_{\min}$ , where their new collision times with, respectively, particles  $j$  and  $j+1$  are computed, and put into the heap, replacing the old ones. As a consequence, the heap has to be re-arranged two more times, again at a cost of at most  $\mathcal{O}(\log N)$  for each modification.

The heap is now again in a consistent state, with the next collision time at the root, and the whole procedure can be repeated. The evolution can be stopped either after some fixed number of collisions  $Z$ , or when the predicted time for the next collision becomes larger than some chosen final time  $T_{\text{end}}$ . In the end, all particles are moved forward in time from their own  $\tau_j$  to the final time which is either  $T_{\text{end}}$  or the time of the last collision. In conclusion, the complexity of the algorithm is in the worst-case  $\mathcal{O}(Z \log N)$  plus lower-order terms  $\mathcal{O}(Z)$  and  $\mathcal{O}(N)$ .

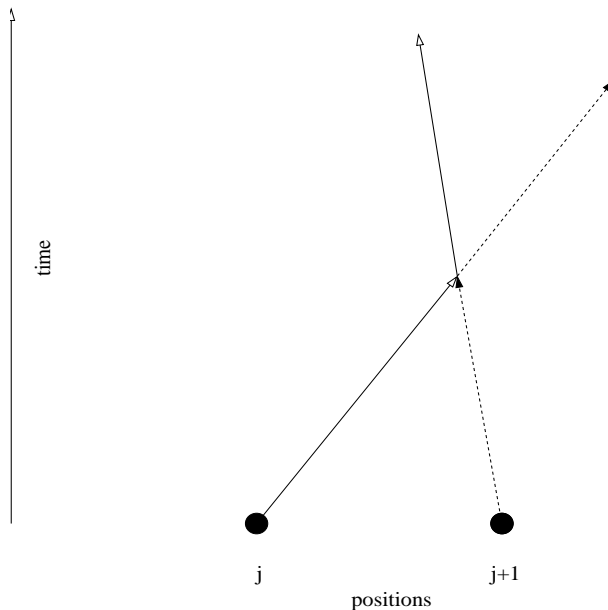


**FIG. 4.** An elastic collision in the  $(x, t)$  plane: the solid line traces the motion of particle  $j$ , while the dashed line shows particle  $j + 1$ .

## 4. APPLICATIONS

In this section we discuss two applications which we have used for testing the performance of the algorithm. In the first, we consider  $N$  freely moving particles in one spatial dimension. The second problem we investigate is the evolution of a Newtonian self-gravitating system in 1- $D$  [2, 3, 12, 19].

### 4.1. Free motion

Consider  $N$  particles all of the same mass  $m$  normalized to be  $N^{-1}$ . Denote the position and the velocity of the  $j$ th particle as respectively  $x_j$  and  $v_j$ . The particles move freely, hence neither interact with each other, nor do they feel any external force. Their acceleration is thus identically equal to zero. In the plane  $(x, t)$ , each particle moves on a straight line, the slope of which is its velocity. The intersection of two lines represents a crossing or a collision in physical space. Each time two particles encounter, i.e.  $x_j = x_{j+1}$ , they cross each other. Equivalently, collisions can be thought of as elastic, since one-dimensional motion of indistinguishable particles is equivalent to a system of one-dimensional impenetrable mass points, which bounce elastically off one another (see Fig. 4). In the latter case, colliding particles exchange their velocities: in the  $(x, t)$  plane the trajectory of a single particle is then a broken line.

We remark that the system of non-interacting particles is not trivial in Eulerian coordinates, and has been used as a model of structure formation in the early Universe, the so-called Zeldovich approximation. Furthermore, as long as the solution stays single-stream, i.e. before any collision has occurred, the Zeldovich approximation is in some sense exact in one dimension [20, 4]. After a first collision, when in the continuum limit a caustic has been formed and the solution is no longer

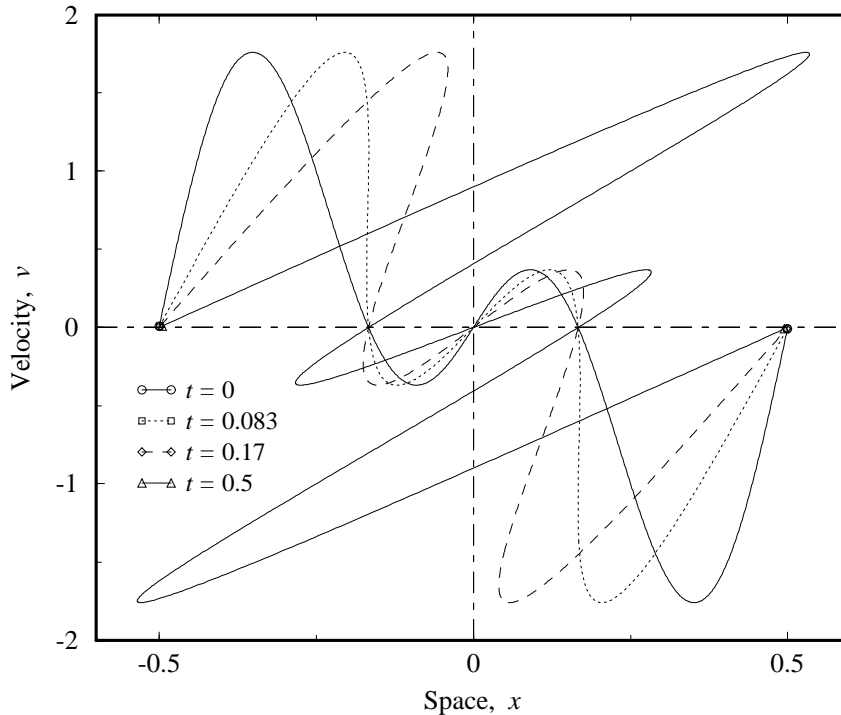


**FIG. 5.** Phase space portraits of the free motion starting from initial velocity on double sine wave. The first caustic is formed at time  $t = (4\pi)^{-1}$  (dotted line). After caustic formation, velocity is a multi-valued function of position and in that region, a Zeldovich pancake, or blini, carries an increasing fraction of the mass.

single-stream, the dynamics of a self-gravitating system can nevertheless be proven to stay close to the Zeldovich approximation for short enough times [14].

Fig. 5 shows a phase-space portrait of this dynamics with particles initially uniformly distributed in space, and velocity a smooth function of position. Fig. 6 shows the same dynamics in the  $(x, t)$  plane, and clearly displays structure formation in Eulerian coordinates (caustics).

#### 4.2. Self-gravitating systems

Consider now a one-dimensional (classical) Newtonian self-gravitating system of  $N$  particles, again all of the same mass  $m = N^{-1}$ . The Hamiltonian is:

$$H = \sum_{j=1}^N \frac{p_j^2}{2m} + 2\pi G m^2 \sum_{j=1}^N \sum_{i>j}^N |x_i - x_j|, \quad (2)$$

where  $x_j$  is the position of particle  $j$ ,  $p_j \equiv mv_j$  is the momentum conjugate to  $x_j$  and  $G$  is the gravitational constant [12, 19]. We choose as unit of length the spatial interval in which the particles are initially contained. The initial density  $\rho_0$  is thus equal to one. The natural choice of time scale is the inverse of the Jeans frequency  $\omega_J = (4\pi G \rho_0)^{1/2}$ . With our choice of length this implies that we take  $4\pi G$  equal to one.

Inbetween two collisions, the acceleration of each particle is constant, and is proportional to the difference of number of particles on its right and on its left. In the



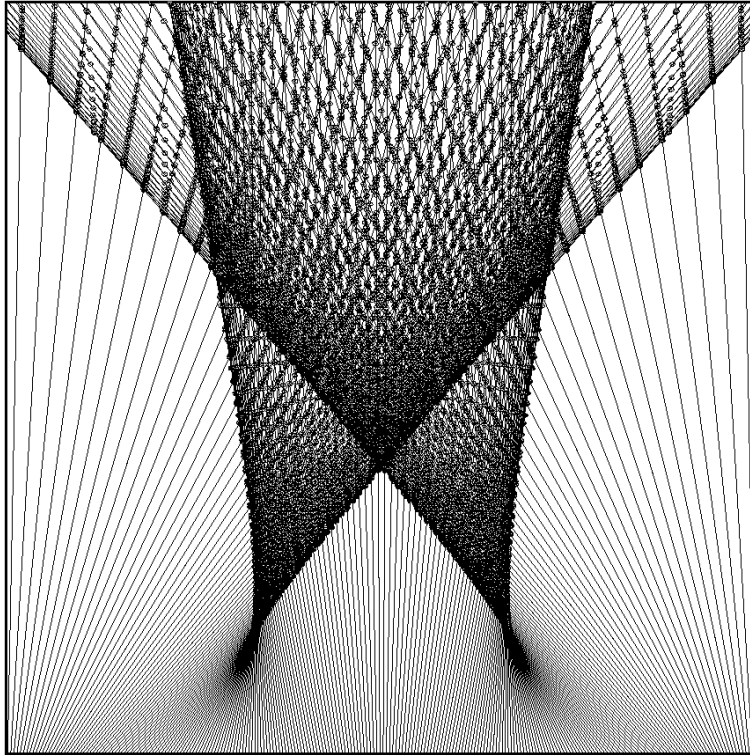


**FIG. 6.** Dynamics in the  $x, t$  plane for free motion with the same initial conditions as Fig. 5. The two caustics are clearly visible. For long times, all particles will fly away to infinity.

$(x, t)$  plane, the path of a particle between collisions thus follows a parabola. If the particles are assumed to pass through each other freely, then in a collision, velocities are unchanged but accelerations are exchanged. If, on the other hand, particles are assumed to scatter elastically, then in a collision, velocities are exchanged but accelerations are unchanged. Switching from one interpretation to the other only involves keeping track of the permutation relating the current rank of the particles to their initial rank. This can be realized algorithmically by bookkeeping at each collision two indexing arrays, inverse of each other in a way similar to the  $HP[\bullet]$  and  $PH[\bullet]$  arrays, but this time holding the relations between the initial and the current particle rank.

Evolving the system thus involves basically two operations: finding the next collision time of a pair of particles and moving these to their common collision time. Although seemingly simple, these two operations contain lots of numerical traps. We remark that the system is chaotic, i.e. dynamically unstable, and amplifies small perturbations. It is thus especially important to keep numerical errors small. First, finding the collision time implies finding the positive root of the quadratic equation

$$\frac{1}{2}\delta a(t_c - t)^2 + \delta v(t_c - t) + \delta x = 0 \quad (3)$$

where  $\delta a$ ,  $\delta v$  and  $\delta x$  are respectively the differences of accelerations, velocities and positions between the right and left particles at the common time  $t$  (so that  $\delta x > 0$  and  $\delta a < 0$ ), and  $t_c$  is their predicted next collision time. That both roots are real and that there can be only one positive root follows from the fact that  $\delta a \delta x$  is negative. As is well known, solving the quadratic equation by the classical formula:

$$t_c - t = \frac{-\delta v \pm \sqrt{\delta v^2 - 2\delta a \delta x}}{\delta a} \quad (4)$$

will lead to severe cancellation when  $\delta v$  is negative,  $\delta x$  is small and the positive root is sought, that is exactly the case that corresponds physically to nearly free motion. Hence we only use (4) when  $\delta v$  is positive and with the  $-$  determination of the radical. When  $\delta v$  is negative, the classical formula can be re-arranged to:

$$t_c - t = \frac{2\delta x}{-\delta v + \sqrt{\delta v^2 - 2\delta a \delta x}} \quad (5)$$

which is stable in this case. Note that both formulas naturally tend to their proper limit when  $\delta a \rightarrow 0$  (the free motion case). In the self-gravitating case and with our choice of units,  $\delta a$  has the constant value  $-N^{-1}$  for neighboring particles.

Second, moving the particles forward in time should be written as

$$x_j(t) = x_j + \left[ v_j + \frac{a_j}{2} (t - \tau_j) \right] (t - \tau_j) \quad (6)$$

that, if  $a_j/2$  is precomputed, involves two nested *fused multiply-add* (**madd**) operations, which on many modern microprocessor are executed in a single clock cycle and with a single roundoff error, leading to a saving of three floating-point operations over the five needed by the classical expression  $x_j + v_j(t - \tau_j) + a_j/2(t - \tau_j)^2$ . Expression (6) can also be recognized as *Horner's rule*, which, even on machines lacking a **madd** instruction, saves one multiplication.

If the positions of two colliding particles are updated according to equation (6), they might end up with a slightly different final position or, even worse, the left particle could overtake the right one because of roundoff. To prevent this we used a common symmetric formula for computing the final position of the pair,

$$\begin{aligned} x_c(t_c) = & \frac{x_j + x_{j+1}}{2} \\ & + \left[ v_j - v_{j+1} + \left( \frac{a_j + a_{j+1}}{2} \right) \left( \frac{\tau_{j+1} - \tau_j}{2} \right) \right. \\ & \quad \left. + (a_j - a_{j+1}) \left( t_c - \frac{\tau_{j+1} + \tau_j}{2} \right) \right] \left( \frac{\tau_{j+1} - \tau_j}{2} \right) \frac{1}{2} \\ & + \left[ v_j + v_{j+1} + \left( \frac{a_j + a_{j+1}}{2} \right) \left( t_c - \frac{\tau_{j+1} + \tau_j}{2} \right) \right] \left( t_c - \frac{\tau_{j+1} + \tau_j}{2} \right) \frac{1}{2} \quad (7) \end{aligned}$$

which is physically equivalent to moving the center of mass of the two particles. Although seemingly complicated, this form is full of repeated subexpressions and can thus be evaluated quite efficiently, especially as it again only involves **madd** operations. This expression also gives the benefit of preserving exactly any symmetries that might be present in the initial velocity profile because positions, velocities and accelerations are combined *before* any multiplication is done.

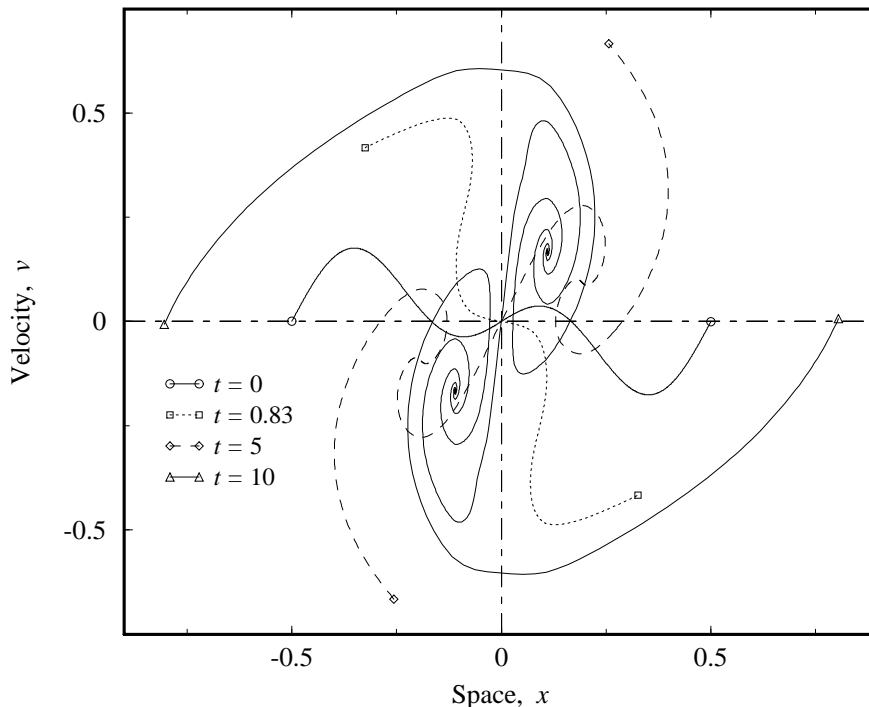
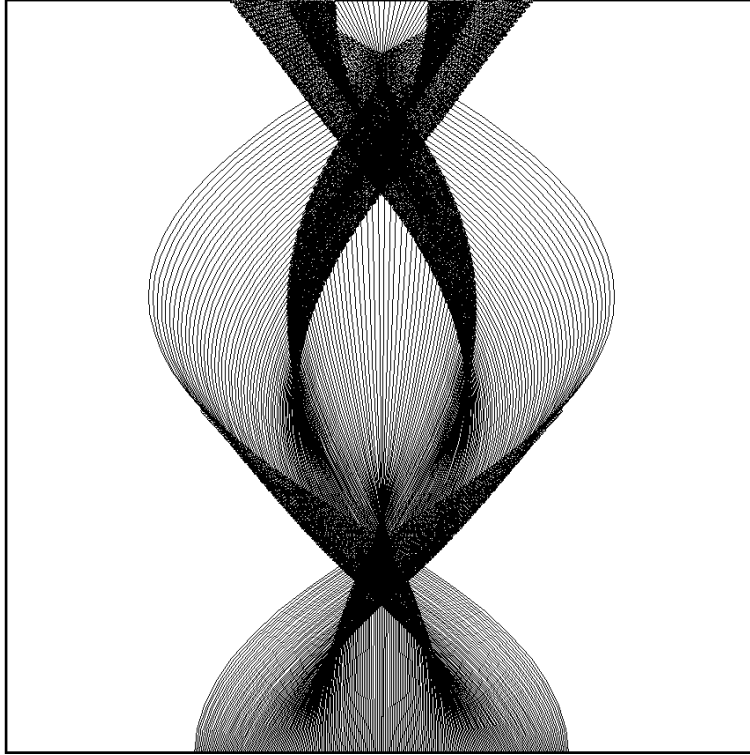


**FIG. 7.** Phase space portrait of a self-gravitating system. The initial velocity profile is the same as in Fig. 7, i.e. a double sine wave. Although the initial evolution is similar to the free motion case, after a few Jeans times, the system develops spiral structures in phase space, due to the gravitational attraction preventing the particles from running away.

Fig. 7 shows phase space portraits of this self-gravitating dynamics with particles initially uniformly distributed in space, and velocity a smooth function of position. After caustic formation, the system develops a spiral structure in phase-space. Fig. 8 shows the same dynamics in the  $(x, t)$  plane. As in free streaming motion, caustics can be observed. In addition, we see that gravitation stops the particles from moving apart as easily after the caustics have been formed and this leads to a more concentrated mass agglomeration. Nevertheless, it is worth stressing the qualitative agreement between Figs. 6 and 8 for the initial stage of the evolution: this is an indirect confirmation of the validity of the Zeldovich approximation.

An event-driven scheme for the simulation of one-dimensional self gravitating systems was first introduced by Eldridge and Feix [3], and has later been further developed in the literature [18]. This and all other published schemes however always involve at least  $\mathcal{O}(N)$  operations per collisions, either to find the minimum collision time, or to update the particle states after each collision. In our algorithm, these two operations need respectively  $\mathcal{O}(\log N)$  and  $\mathcal{O}(1)$  operations.

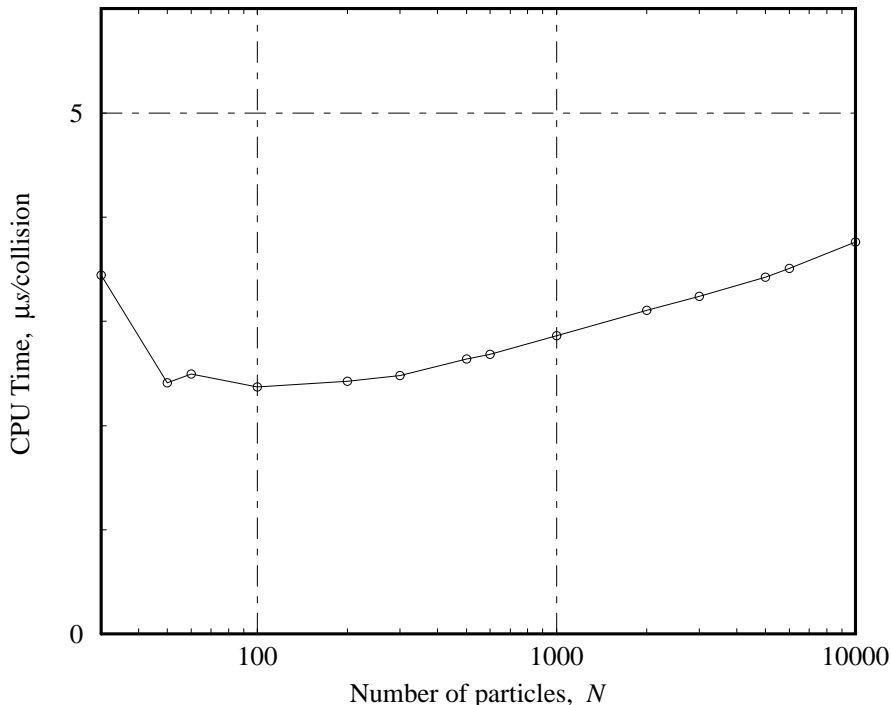
The theoretical predictions of the performance of the algorithm is confirmed by Fig. 9, which shows CPU time per collision *vs.* number of particles in semi-logarithmic scale. The linear dependence on  $\log N$  is clear in the range 300–10000. However, there is a significant constant contribution coming from the floating point operations needed to update the particles states, which actually still take the lion's share of the CPU time for 10000 particles. In the data of Fig. 9 (see caption),



**FIG. 8.** Dynamics in the  $x, t$  plane for a self-gravitating system. For large times, all particles stay trapped in a finite region of space, with their trajectories intermixing each other until the system becomes completely chaotic.

we reached speeds in excess of  $4 \times 10^5$  collisions/s on an inexpensive Linux PC. On a DEC ALPHA-based workstation at 600 MHz, we got speeds of around  $1.3 \times 10^6$  collisions/s, for  $N$  equal to 1000. Hence the algorithm presented here allows the study of fairly large systems for long times on ubiquitous hardware.

The preceding discussion has made clear that a limiting factor for simulating a system up to a given time  $T_{\text{end}}$  is the number of collisions  $Z$  that have to be performed in that time interval. If we want to approach the continuum limit, that is large  $N$ s, it is especially important to know how  $Z$  scales with  $N$ . If  $N$  mass points with total mass equal to one, initially located in an interval of length one, provide a discretization of a given velocity function, then, as long as the discretization is not felt, one expects that the average time between successive collisions of a given particle goes like  $N^{-1}$ . The total collision rate hence grows as  $N^2$ . Likewise, if we consider discretization of a statistically stationary state, the distance between particles would scale as  $N^{-1}$  while the velocity would be independent of  $N$ . Hence, also in this case, the collision rate would be proportional to  $N^2$ . Fig. 10 shows the number of collisions *vs.* time in unit of inverse Jeans' frequency, in double logarithmic coordinates, for different number of particles. The curves corresponding to different  $N$ s are parallel to each other, the separations being the squares of the ratio of successive values of  $N$ . Fig. 10 hence suggests that the proposed scaling holds true for different discretizations of the same initial conditions for all regimes.



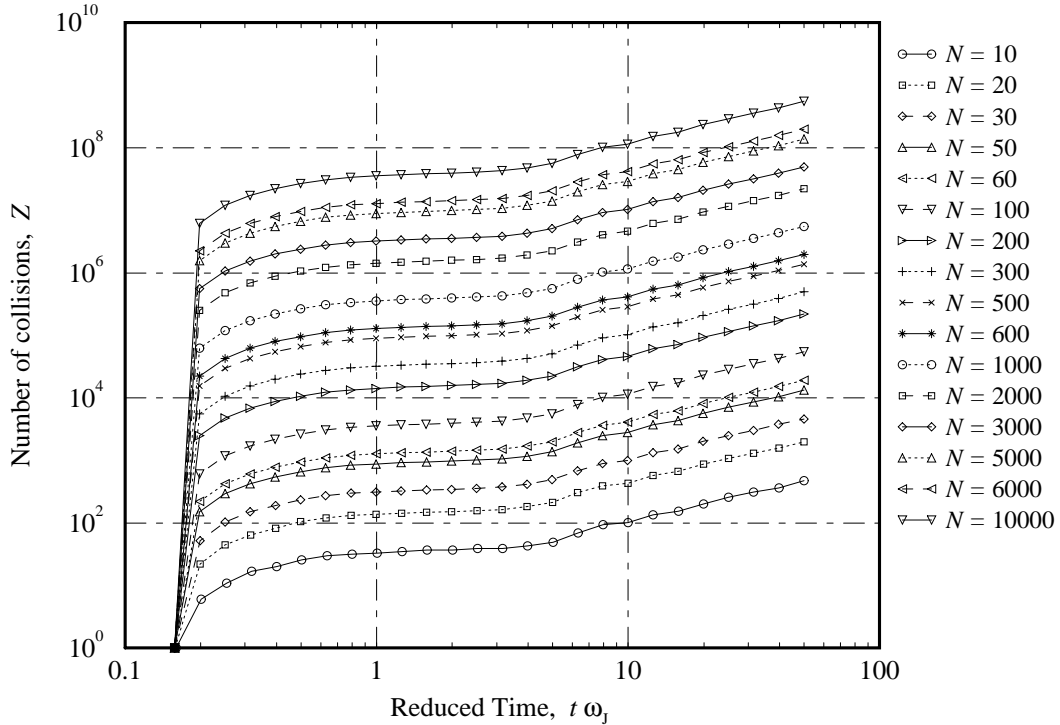
**FIG. 9.** CPU time per collision measured as the output of the UNIX library function `times()`, divided by the number of collisions, after 30 Jeans time, for systems of various size  $N$ . The code was compiled by `gcc` in the Linux kernel 2.2 and ran on an Intel Pentium II 450 MHz processor. Data points on the left are not very reliable because of the limited resolution of `times()`.

Fig. 11 explores the late time regime, and shows the number of collisions *vs.* time in linear scale (the earlier time regimes shown in Fig. 10 are not visible in this representation). It is clear from this figure that the collision rate becomes constant for times much larger than the inverse Jeans' time.

## 5. CONCLUSIONS

We discussed the implementation of a fast heap-based event-driven scheme for integrating numerically one dimensional systems of  $N$  interacting particles, provided the dynamics can be integrated between two successive collisions. The collision times are ordered on a heap, which reduces the complexity to  $\mathcal{O}(\log N)$  operations per collision. As a consequence, for large values of  $N$ , the present algorithm is faster than earlier algorithms in the literature, which are  $\mathcal{O}(N)$ . This opens up the perspective of improving the numerical estimates of the statistics of such systems.

Commonly, a particle system is considered as a discrete approximation to a continuum limit, e.g. self-gravitating particles to the Vlasov-Poisson system of coupled partial differential equations. If so, the main limitation of the present scheme is  $Z$ , the number of collisions needed to be performed in a given (intrinsic) time  $T_{\text{end}}$ . We presented theoretical arguments and numerical simulations showing that  $Z$  generally grows as  $N^2$ . Hence the total computational cost of reaching a time  $T_{\text{end}}$  is  $\mathcal{O}(g(T_{\text{end}})N^2 \log N)$ , where  $g$  is a function depending also on the initial condition, but which becomes proportional to  $T_{\text{end}}$  for sufficiently large  $T_{\text{end}}$ , i.e.  $g \approx f T_{\text{end}}$



**FIG. 10.** Number of collisions *vs.* time in units of  $\omega_j^{-1}$  for different number of particles. We can clearly distinguish one early regime, before many collisions have occurred, one late regime (after about  $10\omega_j^{-1}$ ) where the collision rate becomes constant, and one intermediate regime. For all times, the number of collisions goes as  $N^2$ .

with  $f$  independent of  $N$  and  $\mathcal{O}(1)$  if  $v$  is  $\mathcal{O}(1)$  (see Fig. 11). We believe that one cannot do better for one-dimensional particle systems than the algorithm presented here, without introducing further approximations.

For many applications, such as self-gravitating particles, the system is inherently chaotic, and small errors are amplified by the dynamics. Given some initial accuracy  $\varepsilon$ , the best accuracy that can be got at time  $T_{\text{end}}$  is  $\varepsilon e^{\lambda T_{\text{end}}}$ , for some positive  $\lambda$ . Given this, we might however estimate the relative errors of discretization of a given PDE to a particle system, and the roundoff errors from the collisions, in order to find the “best” value of  $N$  leading to the smallest total error. The first error is essentially  $N^{-1}$ , while the second is  $\eta(f T_{\text{end}} Z/N)^{1/2}$ , where  $\eta$  is the machine precision and  $f T_{\text{end}} Z/N$  is the average number of collisions experienced by a single particle in the interval  $[0, T_{\text{end}}]$ , and the roundoff errors coming from each collision being uncorrelated. The smallest total error is hence found for  $N$  of the order of  $\eta^{-2/3}(f T_{\text{end}})^{-1/3}$  and would thus scale as  $\eta^{2/3}(f T_{\text{end}})^{1/3} e^{\lambda T_{\text{end}}}$ . We see from these expressions that, as expected, the optimal value of  $N$  decreases with  $T_{\text{end}}$ , and that it is useless to use more than  $\approx 10^4$  particles in single precision and more than  $\approx 10^{10}$  in double precision. While the second number of particles is out of reach of current computers, the first one can be handled by our code (about 25 CPU seconds per Jeans time for  $N = 10000$ ). In double precision, we should always use values of  $N$  as large as possible as the limiting value is very large and decreases only very slowly with  $T_{\text{end}}$ .

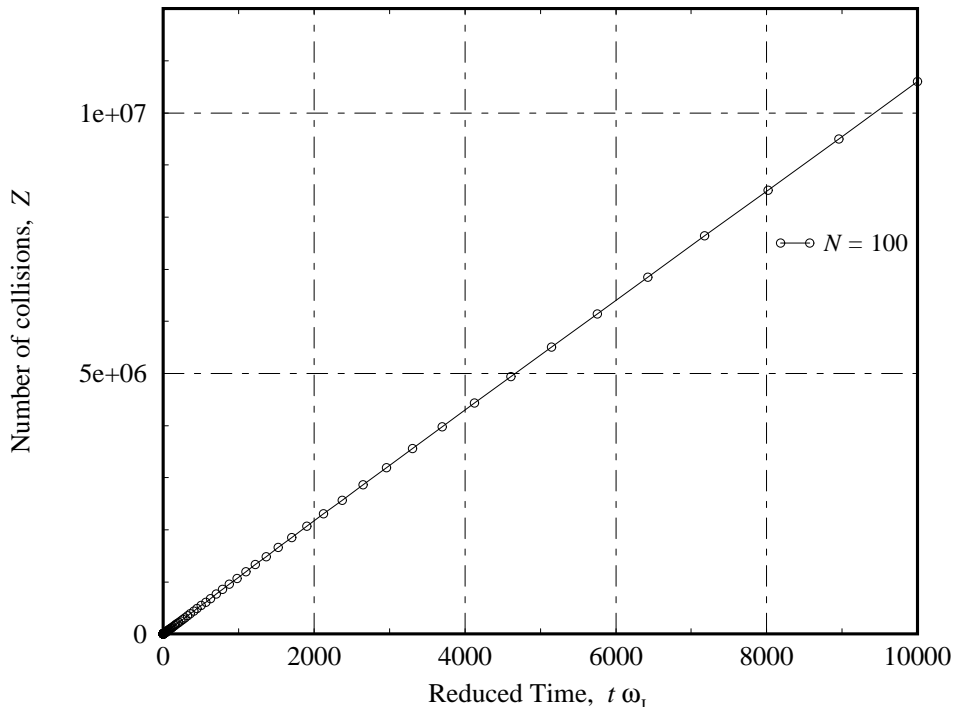


**FIG. 11.** A different representation of Fig. 10, for only one value of  $N$ , but for much longer times and in linear coordinates. The collision rate has clearly become constant at all times displayed in this figure.

It should be added that in both applications presented here, the particle view is at least as fundamental as the PDE one. The discretization gives coarse-grained noise, compared to the PDE, but this is a real physical effect e.g. in stars clusters [5, 11]. Furthermore, for investigation of the statistically steady state in such system, the relevant errors on global quantities are not growing with time in this regime, assuming the validity of the shadowing lemma of dynamical systems theory.

In the paper, we presented free motion and self-gravitating systems as possible applications of our algorithm. Nevertheless, it is worth to stress that the algorithm is more general and, for example, can also be applied to models of the motion of matter in an expanding Universe [1, 15].

### ACKNOWLEDGMENTS

We thank U. Frisch, M. Hénon and P. Muratore-Ginanneschi for discussions. We also thank D. Zanette for pointing out reference [9].

This work was supported by RFBR-INTAS 95-IN-RU-0723 (E.A. and D.F.), by the Swedish Natural Science Research Council through grants M-AA/FU/MA 01778-333 (E.A.) and M-AA/FU/MA 01778-334 (D.F).

### REFERENCES

1. Aurell E., Fanelli D., Muratore-Ginanneschi P., *Physica D*, **148** 272 (2001).
2. Dawson J.M., *The Physics of Fluids* **5**, 445 (1962).
3. Eldridge O.C. and Feix M., *The Physics of Fluids*, **5**, 1076 (1962).

4. Gurbatov S., Malakhov A. and Saichev A. *Nonlinear random waves and turbulence in nondispersive media: waves, rays, particles*, Manchester University Press (1991).
5. Hénon M., *Ann. Astrophys.*, **27**, 82 (1964); *Bull. Astron.*, **3**, 241 (1968).
6. Kingston J.H., *Algorithms and Data Structures - Design, Correctness, Analysis*, Addison-Wesley (1998).
7. Knuth D.E., *The art of computer programming*, Volume 3 **Sorting and Searching**, Addison-Wesley (1973).
8. LaMarca A., and Ladner R.E., *ACM J. Exp. Algorithmics*, **1**, 4 (1996).
9. Marin M., Cordero P., *Comput. Phys. Commun.*, **92**, 214 (1995).
10. Marin M., Risso D. and Cordero P., *J. Comput. Phys.*, **109**, 306 (1993).
11. Meylan G., Heggie D., *Astron. Astrophys. Rev.*, **8**, 1 (1997)
12. Reidl C.J., Miller B.N., *Phys. Rev. A*, **46**, 837 (1992); *Phys. Rev. E*, **48**, 4250 (1993); Miller B.N., Youngkins P., *Phys. Rev. Lett.*, **81** 4794 (1998).
13. Rapaport D.C., *J. Comput. Phys.*, **34**, 184 (1980).
14. Roytvarf A., *Physica D* **73**, 189 (1994).
15. Rouet J.L., M.R. Feix and Navet M., *Vistas in Astronomy*, **33**, 357 (1990); Rouet J.L. et al, *Lecture Notes in Physics: Applying Fractals in Astronomy*, 161 (1991).
16. Sedgewick R., *Algorithms in C*, Addison-Wesley (1990).
17. Sethian J.A., *SIAM Review*, **41-2**, 199 (1999).
18. Severne G., Luwel M., *Astrophys. Space Sci.*, **122**, 299 (1986).
19. Tsuchiya T., Konishi T., Gouda N., *Phys. Rev. E*, **50**, 2607 (1994); Tsuchiya T., Gouda N., Konishi T., *Phys. Rev. E*, **53**, 2210 (1996).
20. Vergassola M., Dubrulle B., Frisch U. and Noullez A., *Astron. & Astrophys.*, **289**, 325 (1993).